Raising forward osmosis brine concentration efficiency through flow rate optimization

Citation: Tow, Emily W., Ronan K. McGovern, and John H. Lienhard V. "Raising Forward Osmosis Brine Concentration Efficiency through Flow Rate Optimization." Desalination 366 (June 2015): 71–79.

As Published: http://dx.doi.org/10.1016/j.desal.2014.10.034

Publisher: Elsevier

Persistent URL: http://hdl.handle.net/1721.1/102499

Version: Author's final manuscript: final author's manuscript post peer review, without publisher's formatting or copy editing

The final version of this manuscript is published in:
Desalination, Vol. 366, p. 71-79 (2015).
http://dx.doi.org/10.1016/j.desal.2014.10.034

Raising forward osmosis brine concentration efficiency through flow rate optimization

Emily W. Tow, Ronan K. McGovern, John H. Lienhard V

Rohsenow Kendall Heat Transfer Laboratory
Department of Mechanical Engineering
Massachusetts Institute of Technology
Cambridge, Massachusetts 02139, USA

Abstract

An exergetic efficiency is defined in order to compare brine concentration processes including forward osmosis (FO) across a wide range of salinities. We find that existing FO pilot plants have lower efficiency than reverse osmosis plants in the brackish and seawater salinity ranges. High salinity FO, in its current form, is still less efficient than mechanical vapor compression. We show that efficiency is the product of FO exchanger and draw regenerator efficiencies, and therefore FO system energy efficiency benefits from improvements to both. The mass flow rate ratio (between draw and feed flow rates) is identified as a crucial parameter in the design of efficient FO systems because of its effect on exchanger efficiency. We demonstrate a method of thermodynamically balancing an FO system by choosing flow rates that lead to equal osmotic pressure differences at both ends of the exchanger, and show the method's potential to increase efficiency by 3-21% based on current system designs.

Keywords: FO, energy consumption, energy efficiency, brine concentration, thermodynamic balancing, high salinity

Nomenclature

A Membrane active layer permeability [m/Pa-s]

*Address all correspondence to *lienhard@mit.edu*

J Water flux [m/s]

K Solute resistivity [s/m]

T Absolute temperature [K]

$\dot{Q}$ Heat transfer rate [W]

$\dot{W}$ Work transfer rate [W]

$\dot{m}$ Mass flow rate [kg/s]

g Specific Gibbs energy [J/kg]

s Salinity or solute mass fraction [kg solute/kg solution]

MR Mass flow rate ratio [-]

MR^* Analytical optimum mass flow rate ratio [-]

RR Recovery ratio [-]

SR Salt consumption ratio [-]

Greek

$\dot{\Xi}$ Exergy flow rate [W]

η Exergetic efficiency [-]

π Osmotic pressure [Pa]

ξ Specific exergy [J/kg]

Subscripts

0 Environment

act Actual

c Concentrated brine

D Osmotic dilution

d Draw stream

dc	Concentrated draw
dd	Diluted draw
F	Fuel
f	Feed
h	Heating fluid
i	In
$least$	Thermodynamic minimum
o	Out
p	Permeate
p'	Fictitious permeate
R	Regenerator
S	Salt
s	Saline stream being concentrated
T	Terminal
X	FO exchanger

1. Introduction

Forward osmosis (FO) is a promising technology for oil and gas (O&G) wastewater treatment [1, 2] because it can concentrate wastewater to high salinities that are currently unattainable with reverse osmosis (RO). In FO, a stream is concentrated as water is drawn from it through a semi-permeable membrane by the high osmotic pressure of a draw solution. Zhao et al. [3] provide a review of the FO process and its applications. FO desalination plants

take FO from a pretreatment process to a desalination system by integrating draw regeneration by thermal or membrane processes. In this paper, we consider FO systems with regeneration except where noted. The efficacy of FO in O&G wastewater desalination has been demonstrated by several pilot plants with varying regeneration systems [2], but energy consumption has yet to be optimized. We will show that reductions in energy consumption may arise from improvements to the FO exchangers, regeneration systems, and system flow rate balance.

Balancing is a method of reducing entropy generation within exchange devices and improving system efficiency through the careful choice of flow rates. Balancing improves gained output ratio (GOR) in humidification dehumidification desalination systems [4, 5, 6, 7, 8] and generally improves efficiency in other applications involving heat and/or mass exchange [9]. Thermodynamically balancing RO, for example, leads to an efficiency improvement of 4.3 percentage points at fixed membrane size and productivity [9]. In the case of FO brine concentration, balancing involves optimizing the ratio of feed and draw flow rates to match osmotic pressure differences on feed and concentrate sides to raise the FO exchanger efficiency, which in turn raises the efficiency of the system.

In this paper, we first evaluate the exergetic efficiency of FO systems and compare them to conventional technologies operating at similar salinities. We then outline an approach to thermodynamically balance the FO exchanger and show the potential of balancing to improve the efficiency of existing FO

pilot plants.

2. Exergetic efficiency of brine concentration

Exergetic efficiency quantifies how much room still exists for reduction of energy consumption in a given process. In this section we define exergetic efficiency for brine concentration processes, and in Sec. 2.1 we assess the efficiency of various processses including FO.

As shown in Fig. 1, a generic FO brine concentration system consists of an FO exchanger, in which brine is concentrated by osmosis as a draw solution is diluted, and a regeneration system, which takes in diluted draw and produces permeate and concentrated draw solution. Although the forward osmosis exchanger consumes minimal energy (in the form of low pressure pump work), the regeneration step is energetically costly.

Exergetic brine concentration efficiency compares the least exergy of separating the saline waste stream into concentrate and permeate (which is a purely thermodynamic quantity) to the actual exergy consumed in the process, which is larger due to irreversibilities in the system. Equation 1 gives the exergetic efficiency, η, of brine concentration:

$$\eta = \frac{\text{least exergy of separation}}{\text{actual exergy consumption}} = \frac{\dot{\Xi}_{least}}{\dot{\Xi}_{act}}. \tag{1}$$

In contrast to the desalination efficiency defined by Mistry and Lienhard [10],

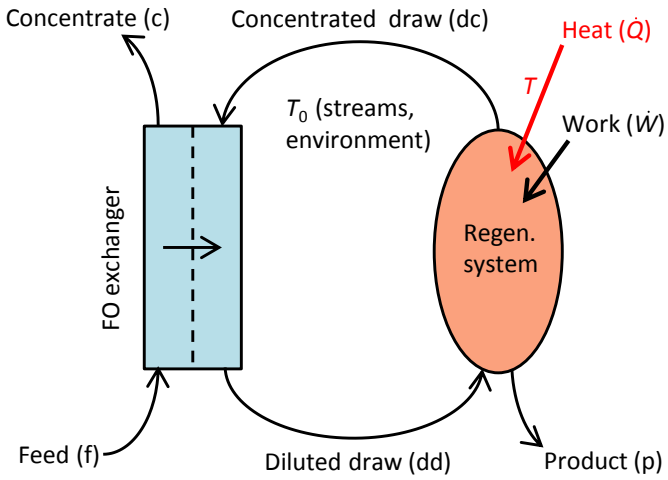

Figure 1: Schematic diagram of an FO desalination system consisting of an FO exchanger and a regeneration system (e.g., RO or distillation). Pre- and post-treatment may also be necessary, but are not considered in this analysis.

which uses the *minimum*[1] least exergy of separating fresh water from a saline stream, the definition employed here uses the least work for a given recovery ratio because in many FO applications (including O&G wastewater treatment) there is value in not only in producing permeate but also in reducing the volume of the feed stream. The exergetic efficiency of brine concentration processes is discussed further in [11]. The least work of separation, $\dot{\Xi}_{least}$, in Eq. 1 is given by Eq. 2 [12] for a system where all streams enter and leave at atmospheric temperature and pressure:

$$\dot{\Xi}_{least} = \dot{m}_p g_p + \dot{m}_c g_c - \dot{m}_f g_f, \tag{2}$$

[1]Corresponding to an infinitesimal recovery ratio, which is defined in Eq. 11.

where $\dot{m}$ and g are mass flow rate and specific Gibbs energy, respectively.

Draw regeneration systems take in exergy in the form of work, heat transfers (HT), and fuel combustion. The actual exergy consumed, $\dot{\Xi}_{act}$, is expanded in Eq. 3:

$$\dot{\Xi}_{act} = \underbrace{\dot{Q}\left(1 - \frac{T_0}{T}\right)}_{\text{isothermal HT}} + \underbrace{\dot{m}_h(\xi_{h,i} - \xi_{h,o})}_{\text{non-isothermal HT}} + \underbrace{\dot{m}_F \xi_F}_{\text{fuel}} + \underbrace{\dot{W}}_{\text{work}}. \tag{3}$$

$\dot{Q}$ is the isothermal heat transfer rate at temperature T (e.g., by condensation of steam), and T_0 is the temperature of the environment. $\dot{m}_h$, $\xi_{h,i}$, and $\xi_{h,o}$ are the mass flow rate, specific exergy in and specific exergy out, respectively, of any non-isothermal heating fluid streams. $\dot{m}_F$ and ξ_F are the mass flow rate and exergetic value of any fuels used. Exergetic values of fuels are given in [13]. $\dot{W}$ is the total work transfer rate (e.g., electrical power).

Substituting Eqs. 2 and 3 into Eq. 1, we can compute the efficiency of any brine concentration system, including FO:

$$\eta = \frac{\dot{m}_p g_p + \dot{m}_c g_c - \dot{m}_f g_f}{\dot{Q}\left(1 - \frac{T_0}{T}\right) + \dot{m}_h(\xi_{h,i} - \xi_{h,o}) + \dot{m}_F \xi_F + \dot{W}}. \tag{4}$$

Equation 4 is used to evaluate the exergetic efficiencies of FO brine concentration systems and conventional desalination methods in the following section.

2.1. Assessment of technologies

The efficiency of brine concentration is visualized in this section with an efficiency-salinity map, Fig. 2. The need for a two-dimensional rating of efficiency stems from the optimization of different processes for particular salinity ranges (e.g., EDR for low-salinity brackish applications) and the effect of salinity on least work of separation.

The values of FO efficiency that appear in the efficiency-salinity map are calculated using the limited FO pilot plant energy consumption data available in the open literature. McGinnis et al. [14] describe the operation of an FO pilot plant that uses an ammonia-carbon dioxide draw solution and thermal draw regeneration to concentrate high-salinity O&G wastewater from the Marcellus and Permian Basin shale regions. This thermal FO pilot uses a distillation column to regenerate the draw, but other thermal draw regeneration types have been proposed or investigated at the lab scale, including mechanical vapor compression (MVC) [14], membrane distillation (MD) [15], and multi-stage flash (MSF) [16]. Thermally-regenerated FO has also been modeled by Semiat et al. [17]. An FO pilot system with RO regeneration (FO-RO) was used to concentrate low-salinity O&G wastewater [2, 18]. FO-RO has also been suggested to be more efficient than RO for seawater desalination [19, 20], but other studies have shown that this is unlikely [21, 22]. Another FO pilot plant forgoes draw regeneration in favor of "osmotic dilution" [2, 18]: the dilution of a pure sodium chloride solution powers the concentration of O&G wastewater. Osmotic dilution is also used

in emergency hydration [23], fertigation [24], and other applications described in [25].

In addition to three existing FO brine concentration pilots, plant efficiency data for seawater RO (SWRO), brackish water RO (BWRO), electrodialysis (EDR), MSF, and high-salinity MVC are included for comparison. Models of seawater FO-RO and high-salinity MVC as well as typical efficiencies of MVC and multi-effect distillation with thermal vapor compression (TVC-MED) are also given. The assumptions made in constructing Fig. 2 are discussed in Appendix A. In Fig. 2, arrows are drawn from the feed salinity to the concentrate salinity at the efficiency of the process.

The efficiency-salinity map (Fig. 2) can be used to choose energy-efficient desalination technologies for specific applications by first locating the desired salinity range on the horizontal axis and then moving up until reaching the most efficient technology.

Figure 2 shows that FO, in its current state, is not the most efficient technology at any salinity. At brackish and seawater salinities, RO is more efficient than FO. Due to irreversible water transport in the FO exchanger, this will probably always be the case [21]. At high salinities, the efficiency of FO with thermal draw regeneration is currently lower that of MVC [11] because of that pilot plant's use of simple distillation for draw regeneration. However, several advanced thermal draw regeneration processes have been proposed [14, 15, 16] that may contribute to raising thermal FO efficiency.

Due to the absence of a regeneration step, the osmotic dilution process has

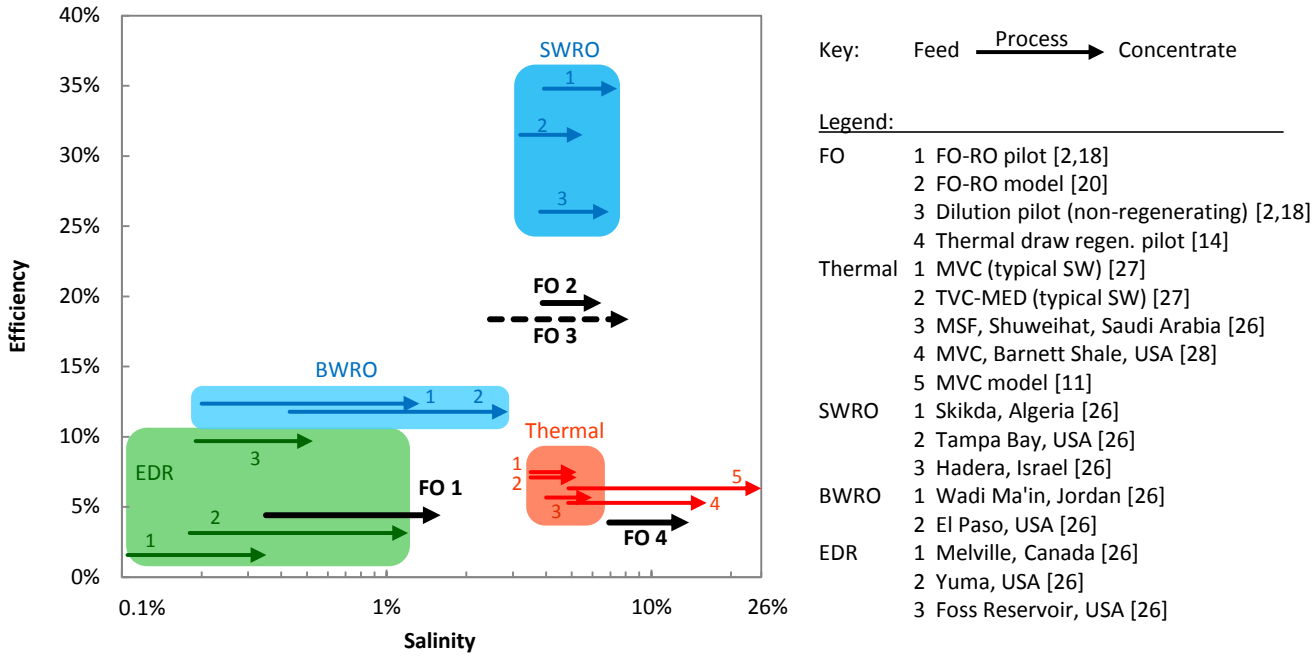

Figure 2: Efficiency-salinity map of desalination processes including FO. Efficiency is calculated with Eqs. 4 and A.1 using data reported in Refs. [2, 11, 14, 18, 20, 26, 27, 28]. Processes are represented with arrows that begin and end at the feed and concentrate salinities, respectively.

a relatively high exergetic efficiency (as defined in Appendix A). However, in the Hutchings et al. pilot [18], at least 75 kg of NaCl must be consumed per cubic meter of water removed from the feed (see Appendix B), and the process produces saline water rather than fresh water. Draw solutes other than NaCl may be used, but in each case the cost of sourcing the solute and the cost of disposing (or value of producing) the dilute draw must be considered. This process might be a good choice for wastewater volume reduction when clean brine production is also desired.

In some cases, the advantages of FO may outweigh its low efficiency. For example, FO is reported to be more resistant to fouling than RO [2, 29, 30], and it has been shown that membrane fouling is more easily reversible in FO than in RO operated under similar conditions [31].

3. FO exchanger efficiency

As it is for most systems, the overall efficiency of an FO brine concentration system is related to the efficiencies of its components. A basic FO system such as that depicted in Fig. 1 consists of two components: an FO exchanger and a draw regenerator. Both components require external exergy inputs: a substantial exergy input in the regenerator, $\dot{\Xi}_R$, and the much smaller power consumption of the FO exchanger, $\dot{W}_X$. The total exergy consumption of the system is $\dot{\Xi}_{act}$, Eq. 3.

The regenerator carries out a separation of the dilute draw solution into permeate and concentrated draw. Here, the least exergy is that of separating

the dilute draw stream (equivalent to the mixing work of combining pure and concentrated draw streams), $\dot{\Xi}_{least,R}$:

$$\dot{\Xi}_{least,R} = \dot{m}_p g_p + \dot{m}_{dc} g_{dc} - \dot{m}_{dd} g_{dd}, \tag{5}$$

and the actual exergy is $\dot{\Xi}_R = \dot{\Xi}_{act} - \dot{W}_X$. Substituting these expressions into Eq. 1 results in the regeneration system efficiency, η_R:

$$\eta_R = \frac{\dot{m}_p g_p + \dot{m}_{dc} g_{dc} - \dot{m}_{dd} g_{dd}}{\dot{\Xi}_{act} - \dot{W}_X}. \tag{6}$$

In systems with regeneration, an FO exchanger efficiency[2] can be defined. Forward osmosis is a spontaneous process, and the transfer of water down a chemical potential gradient is inherently lossy. An exchanger efficiency reflects the exergy destruction in the FO exchanger by comparing the minimum exergy needed to remove water from the feed to the exergy needed to remove the same water from the draw plus the work required by the FO exchanger. The exergetic efficiency of the exchanger can then be expressed as a ratio of the least work of desalinating the feed (Eq. 2) to the least work of separating the draw (Eq. 5) plus the parasitic power consumption associated with

[2]The exchanger efficiency should not be confused with the exchanger effectiveness [32], which quantifies the achieved fraction of water recovery.

overcoming hydraulic losses within the FO exchanger:

$$\eta_X = \frac{\dot{m}_p g_p + \dot{m}_c g_c - \dot{m}_f g_f}{\dot{m}_p g_p + \dot{m}_{dc} g_{dc} - \dot{m}_{dd} g_{dd} + \dot{W}_X}. \tag{7}$$

The exergetic efficiency of the FO unit varies between 0 for no transfer of water and 1 for an ideal exchanger with zero osmotic pressure difference everywhere and no parasitic work consumption. Current pilot plant exchanger efficiencies are in the range of 8-45% (see Sec. 4.2).

The numerator of regenerator efficiency and the denominator of exchanger efficiency are identical (neglecting the parasitic exchanger power consumption) because the draw streams do not cross the system boundary, but only move between components. By relating the component efficiencies to the system efficiency, we can see how changes to each component affect system performance. Using Eqs. 6 and 7, the efficiency a brine concentration system as defined by Eqs. 1 and 2 may be written as a function of the component efficiencies:

$$\eta = \eta_X \eta_R \Big(\frac{\dot{m}_p g_p + \dot{m}_{dc} g_{dc} - \dot{m}_{dd} g_{dd} + \dot{W}_X}{\dot{m}_p g_p + \dot{m}_{dc} g_{dc} - \dot{m}_{dd} g_{dd} + \dot{W}_X \eta_R} \Big). \tag{8}$$

In the case that the hydraulic pressure drop through the FO channels (e.g., 2.8 bar in [14]) is much less than the osmotic pressure of the draw, as would typically occur in FO, $\dot{W}_X \ll \dot{m}_p g_p + \dot{m}_{dc} g_{dc} - \dot{m}_{dd} g_{dd}$ and the system efficiency reduces to Eq. 9:

$$\eta \approx \eta_X \eta_R. \tag{9}$$

Equation 9 shows that the efficiencies of the FO exchanger and the regeneration step are equally important in determining the system efficiency. Regeneration efficiency improvements tend to require increased complexity (e.g., through multistage designs) and/or increased exchanger area (e.g., of RO membrane), both of which add capital cost. Therefore, in the following section we focus on improving the exchanger efficiency inexpensively by optimizing flow rates through the FO exchanger.

4. FO exchanger balancing

FO system efficiency can potentially be raised by improving regeneration, improving the FO exchanger (e.g., through innovation in membranes [33] or draw solutions [34]), or by balancing flow rates throughout the system. Improvements to components can be expensive, but balancing has been shown to raise efficiency at a fixed exchanger area [9]. Therefore, in this section, we will describe thermodynamic balancing as it applies to FO exchangers and quantify its potential to improve FO system efficiency. Parallel-flow exchangers are inherently unbalanced, so only counterflow FO exchangers are considered in this analysis.

Balancing aims to improve the system efficiency at a fixed exchanger area by optimizing the ratio of the mass flow rates entering the exchanger on the draw and feed sides, MR:

$$\mathrm{MR} \equiv \frac{\dot{m}_{dc}}{\dot{m}_f}. \tag{10}$$

Rather than numerically modeling particular systems,we approach bal-

ancing analytically in this section, using fixed terminal osmotic pressure difference as a proxy for fixed exchanger area. The terminal osmotic pressure difference, $\Delta\pi_T$, is the minimum difference between feed and draw stream osmotic pressures at either end of the FO exchanger.[3] As the mass flow rate ratio is varied, $\Delta\pi_T$ is kept constant to minimize the effect on exchanger size and cost.

Recovery ratio defines the mass fraction of the feed that is removed as permeate:

$$\mathrm{RR} \equiv \frac{\dot{m}_p}{\dot{m}_f} = 1 - \frac{s_f}{s_c}. \tag{11}$$

Because of its limited effect on exergetic efficiency, salt permeation through the FO membrane is neglected in this analysis.

Exchanger efficiency (Eq. 7) may be written as a function of MR for a fixed feed salinity, recovery ratio, and terminal osmotic pressure difference. Mass flow rates in Eq. 7 can be normalized by $\dot{m}_f$: $\dot{m}_p/\dot{m}_f = \mathrm{RR}$, $\dot{m}_c/\dot{m}_f = 1-\mathrm{RR}$, $\dot{m}_{dc}/\dot{m}_f = \mathrm{MR}$ and $\dot{m}_{dd}/\dot{m}_f = \mathrm{MR}+\mathrm{RR}$. The Gibbs energy of each stream depends on its salinity (or osmotic pressure). When the minimum osmotic pressure difference occurs at the feed inlet,

$$s_{dd,f} = s_d|_{\pi_f+\Delta\pi_T}, \tag{12}$$

[3]Contrary to the German proverb, *alles hat ein Ende nur die Wurst hat zwei*, a counterflow FO exchanger *also* has two ends with corresponding osmotic pressure differences. The minimum of the two is considered the terminal osmotic pressure difference, $\Delta\pi_T$.

and concentrated draw salinity can be computed with Eq. C.3:

$$s_{dc,f} = \frac{\text{MR+RR}}{\text{MR}}\, s_d|_{\pi_f+\Delta\pi_T}. \tag{13}$$

Similarly, when $\Delta\pi_T$ is at the concentrate side,

$$s_{dc,c} = s_d|_{\pi_c+\Delta\pi_T}, \tag{14}$$

and

$$s_{dd,c} = \frac{\text{MR}}{\text{MR+RR}}\, s_d|_{\pi_c+\Delta\pi_T}. \tag{15}$$

To enforce a minimum terminal osmotic pressure difference of $\Delta\pi_T$, we use a piecewise expression for exchanger efficiency that is the minimum of the efficiencies that would be calculated for minimum osmotic pressure differences occurring at the feed and concentrate sides at a given MR. Therefore, the denominator contains the maximum of the expressions for draw stream mixing work that correspond to the two possible terminal locations of the minimum osmotic pressure difference. Substituting the above relationships into Eq. 7, we arrive at an expression for exchanger efficiency as a function

of MR:

$$\eta_X = [\mathrm{RR}\ g_p + (1-\mathrm{RR})\ g_c - g_f] \times \left(\mathrm{RR}\ g_p + \max\ \left\{ [\mathrm{MR}\ g_d|_{s_{dc,f}} - (\mathrm{MR}+\mathrm{RR})\ g_d|_{s_{dd,f}}], [\mathrm{MR}\ g_d|_{[s_{dc,c}} - (\mathrm{MR}+\mathrm{RR})\ g_d|_{s_{dd,c}}] \right\} + \frac{\dot{W}_X}{\dot{m}_f} \right)^{-1}. \quad (16)$$

In Eq. 16, $s_{dc,f}$, $s_{dd,f}$, $s_{dc,c}$, and $s_{dd,c}$ (Eqs. 12 through 15) are themselves functions of MR.

Exchanger efficiency (Eq. 16) is evaluated in Fig. 3 over a range of mass flow rate ratios to demonstrate the importance of balancing. In Fig. 3, both streams are NaCl solutions, the feed salinity is 8% by mass, the recovery ratio is 50%, and parasitic power consumption is neglected. As the mass flow rate ratio approaches the optimal mass flow rate ratio, the exchanger efficiency rises. Because system efficiency is the product of FO exchanger and regenerator efficiencies (see Eq. 9), any improvement in exchanger efficiency due to balancing results in a roughly proportional improvement in system efficiency for systems with relatively salinity-independent regeneration efficiency.

The sharp peak in efficiency seen in Fig. 3 results from fixing the terminal osmotic pressure difference (which causes the maximum in the denominator of Eq. 16); if instead a fixed exchanger length were imposed, the curves would be smoother.

Conceptually, balancing works by maintaining a relatively uniform os-

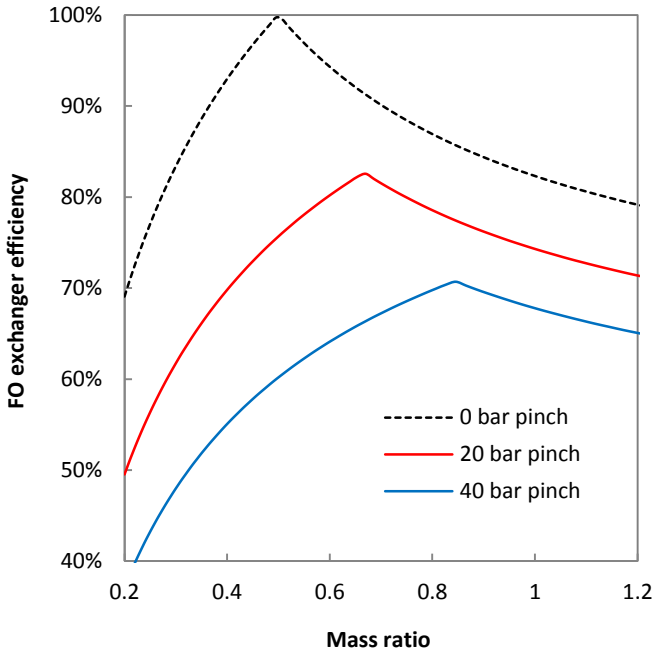

Figure 3: Importance of balancing: FO exchanger efficiency depends on mass flow rate ratio

motic pressure difference throughout the exchanger to minimize entropy generation and maximize efficiency while maintaining sufficient mass flux everywhere. Figure 4 demonstrates the effect of balancing at a fixed terminal osmotic pressure difference (35 bar, based on the low-salinity FO-RO pilot [2, 18]) using salinity profiles derived in Appendix C. As the mass flow rate ratio is varied, the slope of the draw salinity profile changes. Larger mass flow rate ratios lead to a smaller change in draw salinity but require that a larger mass flow rate goes through the regeneration device. Smaller mass flow rate ratios minimize the mass flow rate through the regenerator, but require a larger change in draw salinity. Somewhere in the middle, an optimal mass flow ratio exists that maximizes the exchanger efficiency.

The optimal mass flow rate ratio can be found numerically (as in Fig. 3) or analytically. In general, the mass flow rate ratio is a function of the recovery ratio and the draw salinities at the two ends of the FO exchanger:

$$\mathrm{MR} = \mathrm{RR}\ \frac{s_{dd}}{s_{dc} - s_{dd}}. \tag{17}$$

When MR=MR*,

$$\mathrm{MR}^* = \frac{\mathrm{RR}\ s_d|_{\pi_f + \Delta\pi_T}}{s_d|_{\pi_c + \Delta\pi_T} - s_d|_{\pi_f + \Delta\pi_T}}, \tag{18}$$

the osmotic pressure difference is equal on feed and concentrate sides.

To find the optimal mass flow rate ratio analytically, we examine the effect of MR on η_X, Eq. 7. When the hydraulic pressure drop in the FO exchanger is very small compared to the feed osmotic pressure, as it is in

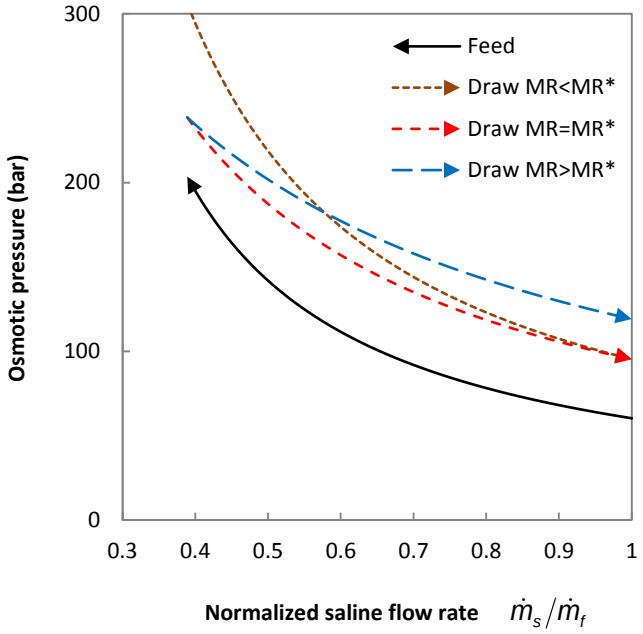

Figure 4: The effect of balancing on the draw salinity profile for an exchanger with $\Delta\pi_T$ = 35 bar. MR = MR* represents an analytically balanced exchanger.

Fig. 5, the change in the parasitic work term in exchanger efficiency ($\dot{W}_X/\dot{m}_f$) with changes in MR is small compared to the change in the mixing work (Eq. 5) of the draw per unit mass of feed, [$\dot{\Xi}_{least,R}/\dot{m}_f = \mathrm{RR}\, g_p + \mathrm{MR}\, g_{dc} - (\mathrm{MR}+\mathrm{RR})\, g_{dd}$]. As shown in Fig. 5, when MR is such that the minimum osmotic pressure difference occurs on the feed side ($\mathrm{MR} \leq \mathrm{MR}^*$), this mixing work decreases with increasing MR, and when $\Delta\pi_T$ is on the concentrate side ($\mathrm{MR} \geq \mathrm{MR}^*$), the mixing work increases with increasing MR. Therefore, the minimum mixing work occurs when the terminal osmotic pressure difference is the same at both ends ($\mathrm{MR} = \mathrm{MR}^*$). Mixing work is in the denominator of exchanger efficiency, and when the parasitic work can be neglected, the expression for MR^* (Eq. 18) is the mass flow rate ratio that maximizes FO exchanger efficiency.

4.1. Limitations

The analytical expression for optimal mass flow rate ratio is based on fixing the terminal osmotic pressure difference and the approximations of low parasitic power consumption and salinity-independent regenerator efficiency. Therefore, Eq. 18 has some limitations.

In low-salinity FO brine concentration, MR^* (Eq. 18) does not predict the optimal mass flow rate ratio, as shown in Fig. 6. Here, the hydraulic pressure loss is significant relative to the feed osmotic pressure, and the variation of the parasitic work term with varying MR cannot be neglected. Numerical optimization, rather than Eq. 18, must be used in low-salinity applications

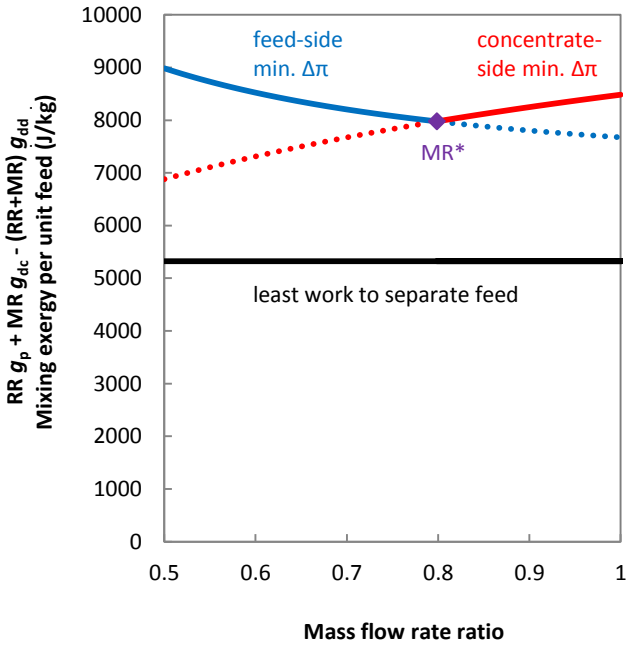

Figure 5: Effect of mass flow rate ratio on the denominator of exchanger efficiency, showing that it is minimized at MR=MR* for a feed salinity of 8% by mass, RR of 50%, 35 bar terminal osmotic pressure difference, and 2 bar hydraulic losses in the exchanger.

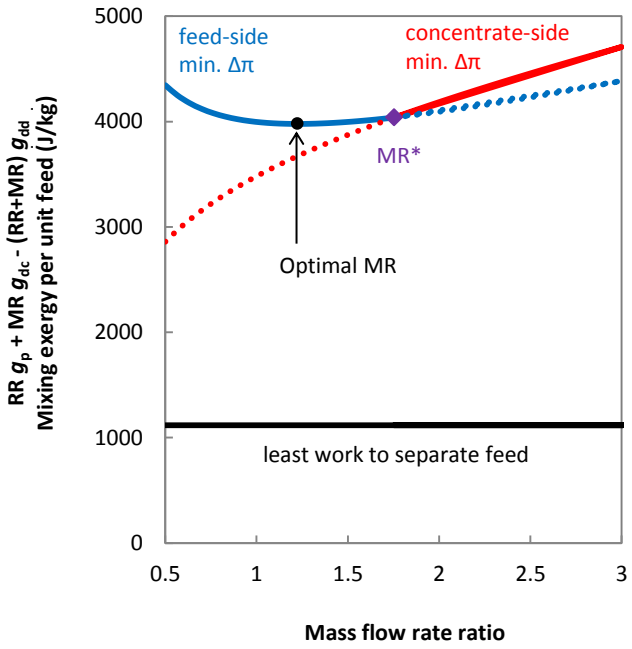

Figure 6: Effect of mass flow rate ratio on the denominator of exchanger efficiency in low salinity operation, showing that the optimal MR occurs below MR*. Here, feed salinity is just 2%, RR is 50%, $\Delta\pi_T = 35$ bar, and hydraulic losses in the exchanger are 2 bar.

such as wastewater treatment with FO membrane bioreactors [35].

Numerical modeling can also be employed to account for internal concentration polarization (ICP), which affects the required membrane area in FO. Assuming operation in FO mode (membrane active layer facing the feed to minimize fouling [36]), and neglecting external concentration polarization, the flux at any point in an FO exchanger is given by Eq. 19 [36]:

$$J = A[\pi_d \exp(-JK) - \pi_s], \tag{19}$$

where J is the water flux into the draw side, A is the membrane active layer permeability, π_d and π_s are the local osmotic pressures of the draw and feed streams, respectively, and K is the solute resistivity of the FO membrane support layer. Eq. 19 shows that the nearly-uniform osmotic pressure difference enforced by Eq. 18 would cause flux to vary throughout the exchanger, which may not be optimal.

Changing the mass flow rate ratio at a fixed terminal osmotic pressure difference requires some change in exchanger area and cost. However, numerically optimizing the mass flow rate ratio at a fixed exchanger area would still improve efficiency according the the theory described in [9]. Analytically balancing the FO exchanger alone also neglects the change in regenerator efficiency with draw salinity, which may be most pronounced with thermal regeneration methods. Future work on numerical modeling of balancing in FO systems could quantify the effect of balancing at a fixed exchanger length including the effects of ICP, parasitic power consumption, and regeneration system efficiency.

4.2. Applications

Optimizing the mass flow rate ratio can improve the efficiency of real systems. In Fig. 7, mass flow rate ratio is varied for the FO exchangers used in the low-salinity FO-RO pilot [2, 18] and the thermal FO pilot [14] as well as the seawater FO-RO model by Nicoll [20]. The osmotic dilution pilot [18] is not included in Fig. 7 because it is more practical to minimize salt

use (see Appendix B) than to maximize exchanger efficiency in the osmotic dilution case. Theoretical exchanger efficiency curves were plotted with the same terminal osmotic pressure difference, feed salinity, and recovery ratio as each pilot plant using Eq. 16. The parasitic electrical consumption of all FO exchangers was estimated based on a 2 bar hydraulic pressure drop in both feed and draw streams. The minimum mass flow rate ratios for the osmotic dilution and thermal FO pilots correspond to a saturated draw solution.[4] The minimum mass flow rate ratios for the low salinity FO-RO pilot and the Nicoll FO-RO model correspond to 7% NaCl draw because they use RO regeneration.

Figure 7 shows the potential of balancing to raise exchanger efficiency in existing systems. The exchanger efficiency varies with mass flow rate ratio (as well as minimum osmotic pressure difference, feed salinity, and recovery ratio, as in Eq. 16), reaching a maximum at MR^* (Eq. 18) in all cases except the low-salinity FO-RO pilot, where the low feed salinity (0.35%) leads to a hydraulic pressure drop comparable to the feed osmotic pressure, as discussed in Sec. 4.1. By choosing the optimal mass flow rate ratio, efficiency improvements of 3% in Nicoll's FO-RO model [20] to 21% in the thermal FO pilot [14] could be realized.

For systems with regeneration processes such as RO whose efficiency is

[4]Properties of the ammonia-carbon dioxide draw solution in [14] were estimated using the extended UNIQUAC model for electrolyte solutions as in [37] with additional data from [38].

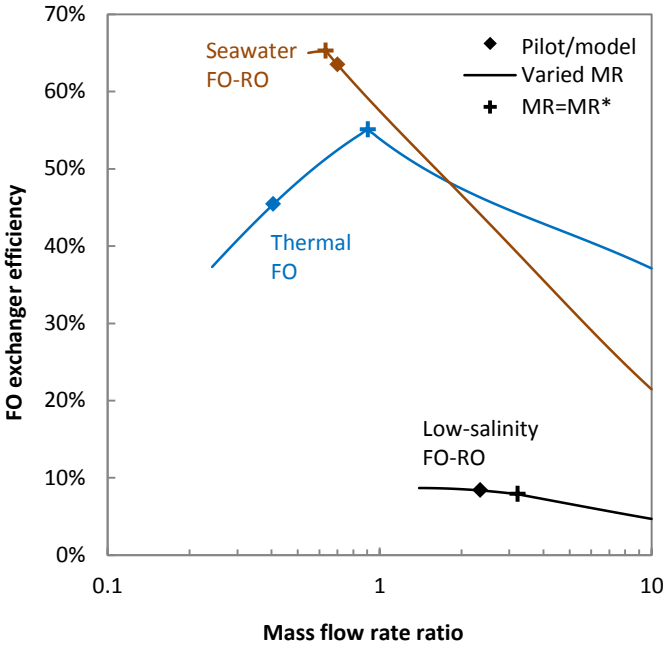

Figure 7: Potential improvements in the FO exchanger efficiency of pilot plants. Mass flow rate ratio is varied for the same terminal osmotic pressure difference, feed salinity, and recovery ratio as each pilot plant using data from [2, 14, 20]. The performance of each plant at its reported mass flow rate ratio as well as at the analytical optimum (MR^*) are also plotted.

relatively independent of feed salinity [11], Eq. 9 shows that the increases in exchanger efficiency due to balancing will be translated into proportional increases in system efficiency. However, the efficiency of thermal regeneration processes may vary more with draw stream salinity, and therefore such systems should be optimized by varying the mass flow rate ratio within a numerical model of the entire system. Either way, the efficiency gain attainable by balancing alone is small, and will not change the trends seen in the salinity-efficiency map (Fig. 2).

5. Conclusion

FO brine concentration processes were compared to established technologies to demonstrate that improvements in exergetic efficiency are needed for FO to become more energetically competitive. We showed that FO system exergetic efficiency is approximately the product of FO exchanger efficiency, which we defined in Eq. 7, and regenerator efficiency. This expression demonstrates that the exchanger and regenerator efficiencies are equally important, and improvements to either will affect the system efficiency proportionally.

The mass flow rate ratio was identified as a crucial parameter in high-efficiency FO system design, and we showed that thermodynamically balancing systems by optimizing the mass flow rate ratio leads to modest improvements in efficiency. We offered a simple expression (Eq. 18) for the optimal mass flow rate ratio that maximizes the FO exchanger efficiency for high salinity FO at a fixed terminal osmotic pressure difference. In the pi-

lot systems considered, balancing by flow rate optimization would improve the exergetic efficiency of FO brine concentration by around 3-21%. In FO desalination system design, the balancing method is best applied by numerically optimizing the mass flow rate ratio for maximum system efficiency at a fixed FO exchanger size, using the analytical expression to provide an initial estimate, and setting the mass flow rates and concentrated draw salinity of the FO system according to the results of the optimization.

6. Acknowledgement

We would like to acknowledge support from the King Fahd University of Petroleum and Minerals through the Center for Clean Water and Clean Energy at MIT and KFUPM (Project #R4-CW-08). We thank Gregory P. Thiel for sharing his implementation of the ammonia-carbon dioxide draw solution property model. Emily acknowledges that this material is based upon work supported by the National Science Foundation Graduate Research Fellowship Program under Grant No. 1122374. Ronan thanks the Hugh Hampton Memorial Fund Fellowship for financial support.

References

[1] T. Pankratz, Fuzzy logic: Oilfield brine management, in: Water Desalination Report, Media Analytics, Houston, TX, pp. 13, 2012.

[2] B. D. Coday, P. Xu, E. G. Beaudry, J. Herron, K. Lampi, N. T. Hancock, T. Y. Cath, The sweet spot of forward osmosis: Treatment of

produced water, drilling wastewater, and other complex and difficult liquid streams, Desalination 333 (2014) 23 – 35.

[3] S. Zhao, L. Zou, C. Y. Tang, D. Mulcahy, Recent developments in forward osmosis: Opportunities and challenges, Journal of Membrane Science 396 (2012) 1 – 21.

[4] G. P. Narayan, J. H. Lienhard V, Thermal design of humidification dehumidification systems for affordable small-scale desalination, IDA Journal 4 (2012) 24–34.

[5] K. M. Chehayeb, G. P. Narayan, S. M. Zubair, J. H. Lienhard V, Use of multiple extractions and injections to thermodynamically balance the humidification dehumidification desalination system, International Journal of Heat and Mass Transfer 68 (2014) 422 – 434.

[6] G. P. Narayan, K. M. Chehayeb, R. K. McGovern, G. P. Thiel, S. M. Zubair, J. H. Lienhard V, Thermodynamic balancing of the humidification dehumidification desalination system by mass extraction and injection, International Journal of Heat and Mass Transfer 57 (2013) 756 – 770.

[7] R. K. McGovern, G. P. Thiel, G. P. Narayan, S. M. Zubair, J. H. Lienhard V, Performance limits of zero and single extraction humidification-dehumidification desalination systems, Applied Energy 102 (2013) 1081 – 1090.

[8] G. P. Thiel, J. H. Lienhard V, Entropy generation in condensation in the presence of high concentrations of noncondensable gases, International Journal of Heat and Mass Transfer 55 (2012) 5133 – 5147.

[9] G. P. Thiel, R. K. McGovern, S. M. Zubair, J. H. Lienhard V, Thermodynamic equipartition for increased second law efficiency, Applied Energy 118 (2014) 292 – 299.

[10] K. H. Mistry, J. H. Lienhard V, Effect of nonideal solution behavior on desalination of a sodium chloride (NaCl) solution and comparison to seawater, Journal of Energy Resources Technology 135 (2013).

[11] G. P. Thiel, E. W. Tow, L. D. Banchik, H. W. Chung, J. H. Lienhard V, Energy consumption in desalinating produced water from shale oil and gas extraction, Desalination (Submitted 2014).

[12] K. H. Mistry, R. K. McGovern, G. P. Thiel, E. K. Summers, S. M. Zubair, J. H. Lienhard V, Entropy generation analysis of desalination technologies, Entropy 13 (2011) 1829–1864.

[13] A. Bejan, Advanced Engineering Thermodynamics, 3rd ed., John Wiley & Sons, Inc., Hoboken, NJ, USA, 2006.

[14] R. L. McGinnis, N. T. Hancock, M. S. Nowosielski-Slepowron, G. D. McGurgan, Pilot demonstration of the NH3/CO2 forward osmosis desalination process on high salinity brines, Desalination 312 (2013) 67 – 74. Recent Advances in Forward Osmosis.

[15] S. Zhang, P. Wang, X. Fu, T.-S. Chung, Sustainable water recovery from oily wastewater via forward osmosis-membrane distillation (FO-MD), Water Research 52 (2014) 112 – 121.

[16] A. Altaee, G. Zaragoza, A conceptual design of low fouling and high recovery FO-MSF desalination plant, Desalination 343 (2013) 2–7.

[17] R. Semiat, J. Sapoznik, D. Hasson, Energy aspects in osmotic processes, Desalination and Water Treatment 15 (2010) 228–235.

[18] N. R. Hutchings, E. W. Appleton, R. A. McGinnis, Making high quality frac water out of oilfield waste, in: Proceedings of the International Society of Petroleum Engineers 2010 Annual Technical Conference and Exhibition, Florence, Italy, September 19-22, 2010.

[19] D. L. Shaffer, N. Y. Yip, J. Gilron, M. Elimelech, Seawater desalination for agriculture by integrated forward and reverse osmosis: Improved product water quality for potentially less energy, Journal of Membrane Science 415-416 (2012) 1–8.

[20] P. Nicoll, Forward osmosis as a pre-treatment to reverse osmosis, in: Proceedings of the International Desalination Association World Congress on Desalination and Water Reuse, Tianjin, China, Oct 20-25, 2013. Paper #TIAN13-121.

[21] R. K. McGovern, J. H. Lienhard V, On the potential of forward osmosis

to energetically outperform reverse osmosis desalination, Journal of Membrane Science 469 (2014) 245–250.

[22] A. Altaee, G. Zaragoza, H. R. van Tonningen, Comparison between forward osmosis-reverse osmosis and reverse osmosis processes for seawater desalination, Desalination 336 (2014) 50 – 57.

[23] E. Butler, A. Silva, K. Horton, Z. Rom, M. Chwatko, A. Havasov, J. R. McCutcheon, Point of use water treatment with forward osmosis for emergency relief, Desalination 312 (2013) 23 – 30.

[24] S. Phuntsho, H. K. Shon, S. Hong, S. Lee, S. Vigneswaran, A novel low energy fertilizer driven forward osmosis desalination for direct fertigation: Evaluating the performance of fertilizer draw solutions, Journal of Membrane Science 375 (2011) 172 – 181.

[25] L. A. Hoover, W. A. Phillip, A. Tiraferri, N. Y. Yip, M. Elimelech, Forward with osmosis: Emerging applications for greater sustainability, Environmental Science & Technology 45 (2011) 9824–9830.

[26] DesalData, desaldata.com/projects, accessed 2014.

[27] D. Hoffman, The application of solar energy for large-scale seawater desalination, Desalination 89 (1992) 115 – 183.

[28] T. Hayes, B. F. Severin, Evaluation of the Aqua Pure Mechanical Vapor Recompression System in the Treatment of Shale Gas Flowback Water:

Barnett and Appalachian Shale Water Management and Reuse Technologies, Technical Report 08122-05.11, Research Partnership to Secure Energy in America, 2012.

[29] C. Klaysom, T. Y. Cath, T. Depuydt, I. F. J. Vankelecom, Forward and pressure retarded osmosis: potential solutions for global challenges in energy and water supply, Chem. Soc. Rev. 42 (2013) 6959–6989.

[30] B. Mi, M. Elimelech, Chemical and physical aspects of organic fouling of forward osmosis membranes, Journal of Membrane Science 320 (2008) 292 – 302.

[31] S. Lee, C. Boo, M. Elimelech, S. Hong, Comparison of fouling behavior in forward osmosis (FO) and reverse osmosis (RO), Journal of Membrane Science 365 (2010) 34 – 39.

[32] L. D. Banchik, M. H. Sharqawy, J. H. Lienhard V, Effectiveness-mass transfer units (epsilon-MTU) model of a reverse osmosis membrane mass exchanger, Journal of Membrane Science 458 (2014) 189 – 198.

[33] N. Y. Yip, A. Tiraferri, W. A. Phillip, J. D. Schiffman, M. Elimelech, High performance thin-film composite forward osmosis membrane, Environmental Science & Technology 44 (2010) 3812–3818.

[34] L. Chekli, S. Phuntsho, H. K. Shon, S. Vigneswaran, J. Kandasamy, A. Chanan, A review of draw solutes in forward osmosis process and

their use in modern applications, Desalination and Water Treatment 43 (2012) 167–184.

[35] A. Achilli, T. Y. Cath, E. A. Marchand, A. E. Childress, The forward osmosis membrane bioreactor: A low fouling alternative to MBR processes, Desalination 239 (2009) 10 – 21.

[36] R. K. McGovern, J. P. Mizerak, S. M. Zubair, J. H. Lienhard V, Three dimensionless parameters influencing the optimal membrane orientation for forward osmosis, Journal of Membrane Science 458 (2014) 104 – 110.

[37] V. Darde, W. J. M. van Well, E. H. Stenby, K. Thomsen, Modeling of carbon dioxide absorption by aqueous ammonia solutions using the extended UNIQUAC model, Industrial & Engineering Chemistry Research 49 (2010) 12663–12674.

[38] D. D. Wagman, The NBS tables of chemical thermodynamic properties: Selected values for inorganic and C1 and C2 organic substances in SI units, American Chemical Society and the American Institute of Physics for the National Bureau of Standards., 1982.

Appendix A. Efficiency assessment methods

Constructing Fig. 2 with data from the open literature required several approximations. In all cases, the permeate was approximated as pure water in the calculation of least work. Also, although water composition varies by

application, the feed was assumed to be a sodium chloride solution in the calculation of least exergy and density. Mistry and Lienhard [10] show that only a small error is introduced when calculating the least work of separation of brackish water and seawater as if they were NaCl solutions. Thiel et al. [11] find that NaCl is a reasonable approximation for the osmotic pressure of high-salinity produced water from the Permian Basin, Marcellus, and Nova Scotia shale plays.

Approximations were also made in calculating exergy consumption. The temperature of heat input in the McGinnis et al. [14] system was assumed to be 100 °C (consistent with the use of atmospheric pressure steam for heating) as in [10], and energy and salinity data was taken from the results of the energy consumption trial in [14]. The recovery ratio of the Shuweihat MSF plant is not reported, so a typical value of 33% [16] was used. 33% recovery was also assumed for seawater TVC-MED and MVC, which are evaluated at 3.5% feed salinity. The RO regeneration step in the low-salinity FO-RO pilot was assumed to be 35% efficient (typical of SWRO systems) because of the 4.5% salinity of the diluted draw. The flow rate through the RO unit was calculated based on conservation of salt and water for the stream salinities given in [2]. The Nicoll seawater FO-RO model [20] assumed a terminal osmotic pressure difference of 1.6 bar, which would require an extraordinarily large membrane area (see Eq. 19).

Evaluating the efficiency of the non-regenerating ("osmotic dilution") FO brine concentration system described by Hutchings et al. [18] in such a way

that it could be compared to regenerating systems was not straightforward because the plant did not produce pure water. To make this comparison, we borrowed the FO exchanger efficiency defined in Sec. 3 (Eq. 7) for exchangers within regenerating systems, which relates the least work of separating the feed, as given by Eq. 2, to the least exergy required to regenerate the draw (Eq. 5) plus the work required to overcome hydraulic losses in the exchanger, $\dot{W}_X$. The osmotic dilution FO efficiency used to compare the Hutchings et al. plant [18] to processes that produce permeate in Fig. 2 is given in Eq. A.1:

$$\eta_D = \frac{\dot{m}_{p'} g_{p'} + \dot{m}_c g_c - \dot{m}_f g_f}{\dot{m}_{p'} g_{p'} + \dot{m}_{cd} g_{cd} - \dot{m}_{dd} g_{dd} + \dot{W}_X}. \tag{A.1}$$

Subscripts dc and dd refer to the concentrated and dilute draw solutions, respectively. The subscript p' refers to the water that moves from the stream being concentrated to the draw stream. Under the assumption of no salt permeation, $\dot{m}_{p'} = \dot{m}_f - \dot{m}_c$ and $g_{p'}$ is the pure water Gibbs energy.

Appendix B. Salt consumption in osmotic dilution

In osmotic dilution systems, reasonably high efficiency is balanced by high salt consumption. Therefore, predicting and minimizing the salt consumption is critical. Although the aforementioned pilot plant consumed a saturated salt solution [2, 18], salt use could be minimized in the osmotic dilution system shown in Fig. B.8, which takes in only solid salt. In a continuous, counterflow system of this type, part of the dilute draw is internally

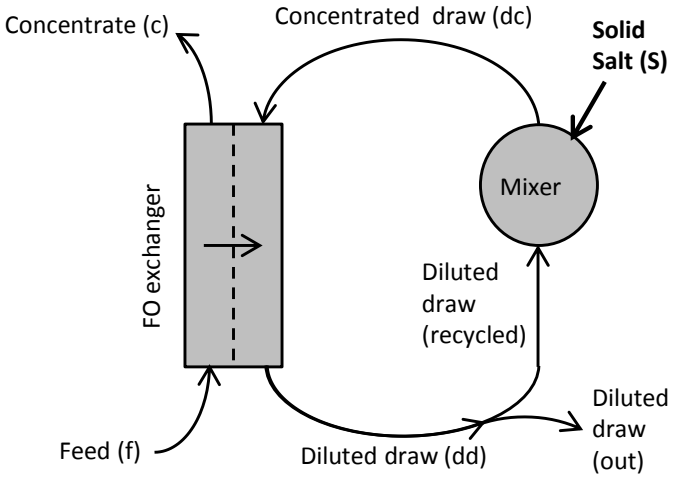

Figure B.8: Osmotic dilution brine concentration system that consumes solid salt

recycled to make the concentrated draw.

We can define a dimensionless performance parameter, the salt ratio SR, which gives the mass of salt consumed per unit mass of water removed from the feed:

$$\mathrm{SR} \equiv \frac{\dot{m}_S}{\dot{m}_{p'}}. \tag{B.1}$$

Taking conservation of water and salt on the draw side of the system in Fig. B.8, we find that the salt ratio is:

$$\mathrm{SR} = \frac{s_{dd}}{1 - s_{dd}}, \tag{B.2}$$

where s_{dd} is the salinity of the dilute draw stream.

By Eq. B.1, the salt ratio of the osmotic dilution pilot [2] would be 0.075 (75 g NaCl per kg water removed from the feed) based on its dilute draw

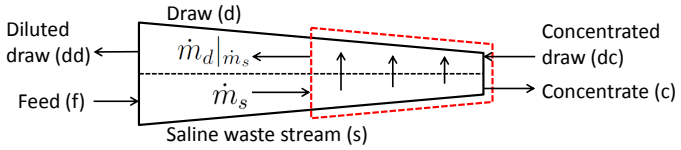

Figure C.9: Schematic diagram of counterflow FO exchanger for balancing analysis

salinity of 7% [2]. This differs from the system described by Mistry and Lienhard [10] which used the energy of solvation for a salt to power the separation of pure water from saline water. The osmotic dilution system described here consumes less salt per unit water removed from the feed, but it does not produce pure water. Because the salt ratio (Eq. B.2) is only a function of dilute draw salinity, an osmotic dilution system of this type does not benefit from balancing, and only requires that the minimum osmotic pressure difference occurs at the feed side ($\mathrm{MR} \leq \mathrm{MR}^*$).

Appendix C. Salinity profile analysis

Figure C.9 illustrates a control volume analysis of an FO exchanger with a saline stream to be concentrated (subscript s) and a draw stream (subscript d). Mass flow rates and salinities at the feed and concentrated draw inlets are known. Salinities and mass flow rates inside the exchanger are determined as functions of the saline stream mass flow rate, $\dot{m}_s$, at any point in the exchanger, neglecting concentration polarization. These profiles are illustrated in Fig. 4.

Making a control volume of the saline side of the FO exchanger in Fig. C.9,

conservation of salt determines the salinity as a function of mass flow rate, assuming no salt permeation:

$$s_s|_{\dot{m}_s} = \frac{s_f \dot{m}_f}{\dot{m}_s}. \tag{C.1}$$

Conservation of salt in the draw-side of the FO exchanger, $\dot{m}_d|_{\dot{m}_s}\, s_d|_{\dot{m}_s} = \dot{m}_{dc} s_{dc}$, along with conservation of mass in the control volume with a dashed outline in Fig. C.9, $\dot{m}_s + \dot{m}_{dc} = \dot{m}_c + \dot{m}_d|_{\dot{m}_s}$, leads to the salinity in the draw side as a function of saline stream mass flow rate, Eq. C.2:

$$s_d|_{\dot{m}_s} = \frac{s_{dc}\dot{m}_{dc}}{\dot{m}_{dc} + \dot{m}_s - \dot{m}_c}. \tag{C.2}$$

Evaluating Eq. C.2 at the dilute draw outlet (feed inlet), we find the relationship between dilute and concentrated draw salinities as function of RR and MR, which are defined in Sec. 4:

$$\frac{s_{dd}}{s_{dc}} = \frac{\dot{m}_{dc}}{\dot{m}_{dd}} = \frac{\mathrm{MR}}{\mathrm{MR} + \mathrm{RR}} \tag{C.3}$$